Article

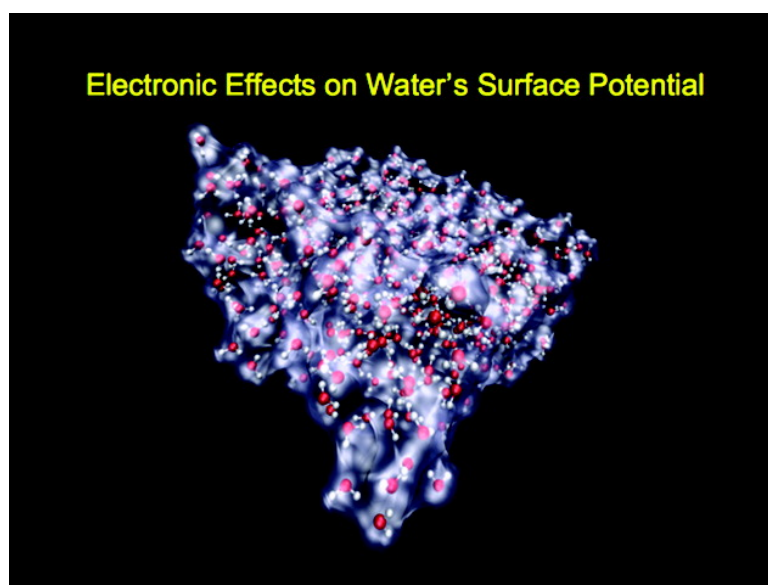# Electronic Effects on the Surface Potential at the Vapor#Liquid Interface of Water

Shawn M. Kathmann, I-Feng William Kuo, and Christopher J. Mundy

More About This Article

Additional resources and features associated with this article are available within the HTML version:

- Supporting Information
- Access to high resolution figures
- Links to articles and content related to this article
- Copyright permission to reproduce figures and/or text from this article

View the Full Text HTML

Electronic Effects on the Surface Potential at the Vapor−Liquid Interface of Water

Shawn M. Kathmann,*,[†] I-Feng William Kuo,[‡] and Christopher J. Mundy[†]

Chemical and Materials Sciences Division, Pacific Northwest National Laboratory, Richland, Washington 99352, and Chemical Sciences Division, Lawrence Livermore National Laboratory, Livermore, California 94550

Received April 17, 2008; E-mail: shawn.kathmann@pnl.gov

Abstract: The surface potential of the vapor−liquid interface of pure water is relevant to electrochemistry, solvation thermodynamics of ions, and interfacial reactivity. The chemistry of an ion near the vapor−liquid interface is influenced by the surface potential. Indirect determinations of the surface potential have been experimentally attempted many times, yet there has been little agreement as to its magnitude and sign (-1.1 to $+0.5$ V). We present the first computation of the surface potential of water using ab initio molecular dynamics and find a surface potential of -18 mV with a maximum interfacial electric field of $+8.9 \times 10^7$ V/m, which are consistent with structural data from experiment. A comparison is made between our results and those from experiments and previous molecular simulations. The associated electric field can alter interfacial reactivity and transport, while the surface potential can be used to determine the "chemical" contribution to the real and electrochemical potentials for ion transport through the vapor−liquid interface.

I. Introduction

The average molecular structure of the vapor−liquid interface is different from the liquid phase because of the broken symmetry provided by the interface. The electrodynamics of the vapor−liquid interface of pure water is relevant to electrochemistry, ion interfacial transport, solvation thermodynamics of ions, and interfacial reactivity.[1−19] The chemistry of an ion near the vapor−liquid interface is influenced by the surface potential (χ). Gas-phase ions, even when not directly important, provide a fundamental standard state for understanding bulk and interfacial solvation and chemistry. The current study provides deeper insight into the surface potential at the vapor−liquid interface of pure water.

Much confusion has surrounded the quantification of the water vapor−liquid surface potential. We consider two routes to the surface potential: (1) thermodynamics and (2) electrodynamics. Along the thermodynamic route, Pratt[12,20] and Zhou, Stell, and Friedman[21] have shown that as long as there are a few trace ions in the system, there is an ionic contribution to the surface potential that does not vanish as one approaches the limit of infinite dilution. A simple way of conceptualizing this trace-ion effect is that even though the bulk concentration of ions may be small, the surface concentration may be appreciable. Pratt[12] has discussed the difficulties arising from the thermodynamic formulation of the surface potential because of its definition in terms of the chemical potentials of ion pairs in the appropriate phases (see refs 12 and 21 for details regarding the thermodynamic treatment). As a further complication of the issue, Pratt noted that there is an apparent dependence of the limiting value of this ionic contribution on the compositional path taken to infinite dilution; this dependence arises from kinetic barriers hindering the transport and equilibration of ions. The key point is how the compositional dependence of the surface potential approaches the pure liquid: in general, this approach is not monotonic, and the approach from concentrated solution to pure water can be quite different (nonlinear) depending on the chemical nature of the solute ions. Furthermore, the concentrated-solution surface potential can approach from both above and below the surface potential of pure water. In the electrodynamic definition, the surface potential is determined by averaging over the underlying spatial charge distribution. This is in stark contrast to the surface potential

[†] Pacific Northwest National Laboratory.
[‡] Lawrence Livermore National Laboratory.
(1) Croxton, C. *Statistical Mechanics of the Liquid Surface*; John Wiley & Sons: New York, 1980.
(2) Motakabbir, K. A.; Berkowitz, M. L. *Chem. Phys. Lett.* **1991**, *176*, 61.
(3) Schweighofer, K. J.; Benjamin, I. *Chem. Phys. Lett.* **1993**, *202*, 379.
(4) Dang, L. X.; Chang, T.-M. *J. Phys. Chem. B* **2002**, *106*, 235.
(5) Lamoureaux, G.; Roux, B. *J. Phys. Chem. B* **2006**, *110*, 3308.
(6) Wilson, M. A.; Pohorille, A.; Pratt, L. R. *J. Chem. Phys.* **1988**, *88*, 3281.
(7) Wilson, M. A.; Pohorille, A.; Pratt, L. R. *J. Phys. Chem.* **1987**, *91*, 4873.
(8) Stillinger, F. H.; Ben-Naim, A. *J. Chem. Phys.* **1967**, *47*, 4431.
(9) Sokhan, V. P.; Tildesley, D. J. *Mol. Phys.* **1997**, *92*, 625.
(10) Randles, J. E. B.; Schiffrin, D. J. *J. Electroanal. Chem.* **1965**, *10*, 480.
(11) Randles, J. E. B. *Phys. Chem. Liq.* **1977**, *7*, 107.
(12) Pratt, L. R. *J. Phys. Chem.* **1992**, *96*, 25.
(13) Koryta, J.; Dvorak, J.; Kavan, L. *Principles of Electrochemistry*; John Wiley & Sons: New York, 1993.
(14) Gomer, R.; Tryson, G. *J. Chem. Phys.* **1977**, *66*, 4413.
(15) Goh, M. C.; Hicks, J. M.; Kemnitz, K.; Pinto, G. R.; Bhattacharyya, K.; Eisenthal, K. B.; Heinz, T. F. *J. Phys. Chem.* **1988**, *92*, 5074.
(16) Farrell, J. R.; McTigue, P. *J. Electroanal. Chem.* **1982**, *139*, 37.
(17) Eley, D. D.; Evans, M. G. *Trans. Faraday Soc.* **1938**, *34*, 1093.
(18) Bard, A. J.; Faulkner, L. R. *Electrochemical Methods: Fundamentals and Applications*; John Wiley & Sons: New York, 1980.
(19) Adamson, A. W. *Physical Chemistry of Surfaces*; John Wiley & Sons: New York, 1990.
(20) Pratt, L. R.; Pohorille, A. *Chem. Rev.* **2002**, *102*, 2671.
(21) Zhou, Y.; Stell, G.; Friedman, H. L. *J. Chem. Phys.* **1988**, *889*, 3836.
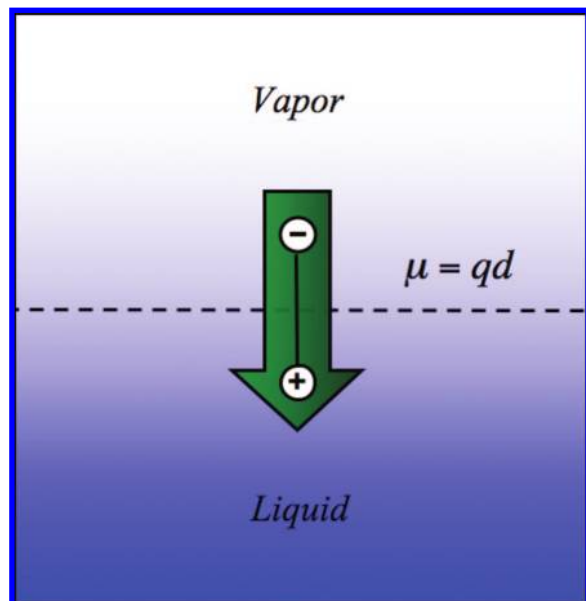
Figure 1. Illustration of the conventional view of the positive surface potential of water ($\chi > 0$) arising from water's dipole moment μ ($\mu = qd$, where q is the charge and d is the distance between the positive and negative poles), which points from the vapor (top) into the liquid (bottom). The surface potential arises from the polar properties of the water molecules and their orientation with respect to one another in the surface region (dashed line).

defined thermodynamically in terms of equilibrium chemical potentials of ions with the total system constrained by electroneutrality. It has not been possible to directly measure the surface potential of pure water[11,12] in either the thermodynamic or electrodynamic sense. Indirect evidence has been used to estimate χ thermodynamically, but the results (-1.1 to $+0.5$ V) do not provide a consistent sign much less a magnitude for χ. In contrast, using an electrodynamic approach, Pratt[12,22] has suggested that use of neutron scattering in conjunction with electron reflectivity experiments may provide a more consistent picture of the atomic structure and charge distribution of the vapor–liquid interface. However, he cautions that such experiments may be exceedingly difficult to perform and interpret. As a point of research, future studies[23] should quantify this "phantom ionic effect" to determine its relevance to the surface potential. In any case, the surface potential at the vapor–liquid interface of pure water is of fundamental importance and can be explored computationally using electrodynamics.

Before getting to the electrodynamic treatment, we note that the surface potential χ at the vapor–liquid interface of water has conventionally[26] been thought to have a positive sign arising from the hydrogen atoms pointing into the liquid to produce a net dipole (see Figure 1). This view was supported by early interpretations of surface spectroscopic measurements,[15] computer simulations,[8] and interpretations of temperature-dependent electrochemical cell experiments.[11] This line of reasoning will be addressed more directly, after we present some additional background.
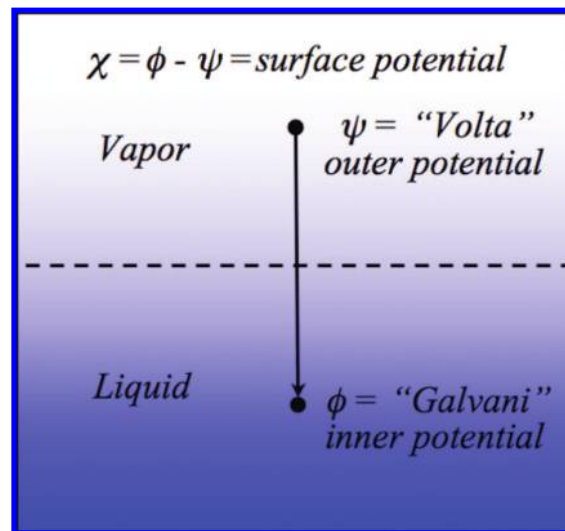
(22) Parfenyuk, V. I. *Colloid J.* **2002**, *64*, 588.
(23) Levin, Y. *J. Chem. Phys.* **2008**, *129*, 124712.
(24) Mortensen, J. J.; Parrinello, M. *J. Phys. Chem. B* **2000**, *104*, 2901.
(25) Deleted in proof.
(26) Girault, H. H. *Analytical and Physical Electrochemistry*; Marcel-Dekker, Inc.: New York, 2004.

Figure 2. Illustration showing the connection between the "Volta" outer potential ψ, the "Galvani" inner potential ϕ, and the surface potential $\chi = \phi - \psi$ at the interface (dashed line) between the vapor (top) and liquid (bottom).

The surface potential χ is generally defined[13,18,19,27] (see Figure 2) as the difference between the liquid-phase "Galvani" inner potential ϕ and the vapor-phase "Volta" outer potential ψ and is given by

$$\chi = \phi - \psi \qquad (1)$$

The Volta outer potential can be determined from the work required to bring an unperturbing unit charge from infinity to a point just outside the vapor–liquid interface. Similarly, the Galvani inner potential could be determined from the work required to bring an unperturbing unit charge from infinity through the vapor–liquid interface into the bulk liquid. In practice, however, the work required to move a charge through an interface must involve a real physical charge, i.e., an electron or an ionic atom or molecule. The motion of a physical charge through the vapor–liquid interface is associated with changes to the interfacial structure and electronic environment. From thermodynamics, the "electrochemical" potential η_i associated with the process of moving charged species i from infinity to the surface, through the vapor–liquid interface, and then into the bulk liquid can be divided into "chemical", "real", and "electrostatic" contributions (sometimes called an extrathermodynamic assumption) as follows:[13,18,19]

$$\eta_i = \mu_i + z_i\phi = \mu_i + z_i\chi + z_i\psi = \alpha_i + z_i\psi \qquad (2)$$

where μ_i is the chemical potential, $\alpha_i = \mu_i + z_i\chi$ is the real potential, and z_i is the charge of the ion. Since these distinctions can be quite confusing, we offer an alternative point of view: the electrochemical potential η_i can be conceptualized as the inhomogeneous chemical potential (in the sense of the reversible work required to move an ion between two phases), whereas the chemical potential μ_i can be thought of as the homogeneous chemical potential (i.e., the reversible work required to create an ion in a single phase).

As Wilson et al.,[6,7] Pratt,[12] and others[9,28] have pointed out, molecular-level simulations hold the promise of being able to directly determine the surface potential χ of the vapor–liquid

(27) Fawcett, W. R. *Liquids, Solutions and Interfaces: From Macroscopic Descriptions to Modern Microscopic Details*; Oxford University Press: New York, 2004.
(28) Jungwirth, P.; Tobias, D. J. *Chem. Rev.* **2006**, *106*, 1259.
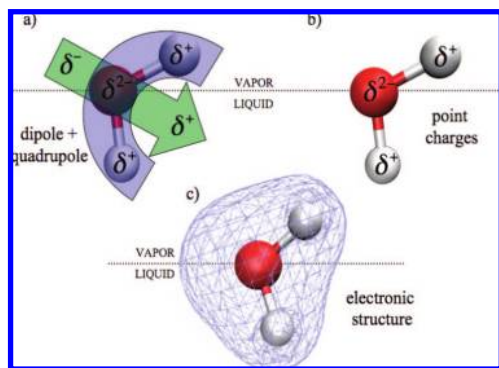
Figure 3. Illustration of various levels of approximation used in treating the spatial charge density of water molecules at the vapor−liquid interface: (a) dipole (green) and quadrupole (blue) moments, (b) partial point charges, and (c) electronic structure charge distribution. (These images are for illustrative purposes only and thus do not reflect the true orientations of the water molecules at the vapor−liquid interface.)

Table 1. Comparison of Surface Potentials χ for Various Water Models[9] at 298 K: The Quantum-Mechanical Surface Potential Including Electronic Degrees of Freedom Is Quite Different from Empirical Interaction Potentials for Water, but the Sign Is Consistently Negative

water model	χ (mV)
this work	−18
TIP4P	−510
D-C	−480
SPC/E	−546
SPC	−530
CC	−600
RWL	−530
TIPS2	−890

interface of pure water. Thus, if the surface potential χ can be calculated independently, then the chemical potential μ_i of the ion can be obtained and used in closure calculations[29] for consistency with measurements of the electrochemical potential η_i as well as other interfacial measurements, such as second harmonic generation[15] or vibrational sum frequency spectroscopy.[30] From electrodynamics, the surface potential χ of the vapor−liquid interface may be calculated by integrating the total interfacial electric field $E_z(z)$ across the vapor−liquid interface:

$$\chi = \varphi(z_{inner}) - \varphi(z_{outer}) = -\int_{z_{outer}}^{z_{inner}} E_z(z')\,\mathrm{d}z' \quad (3)$$

where $\varphi(z_{inner}) = \phi$, $\varphi(z_{outer}) = \psi$, and z is taken to be positive as one moves from the vapor ($z_{outer} = 0$ Å) to the liquid phase ($z_{inner} = 35.7$ Å); only the z component is relevant since the x and y contributions sum to zero by symmetry. Similarly, the interfacial electric field is obtained by integrating $\langle\rho(z)\rangle$, the total charge density averaged over the full ab initio molecular dynamics (MD) trajectory, across the vapor−liquid interface:

$$E_z(z_{outer}) - E_z(z_{inner}) = 4\pi\int_{inner}^{outer} \langle\rho(z')\rangle\,\mathrm{d}z' \quad (4)$$

As might be anticipated, the interfacial electric field $E_z(z)$ and surface potential χ are sensitive functions of $\rho(z)$.

The central issue that is most relevant to the accurate calculation of the electrostatic potential $\varphi(z)$ as a function of z is how to represent the spatial charge density $\rho(z)$ in condensed matter. Previous studies[9,22] and reviews[12,28] discuss the approximation of the spatial charge density of each water molecule by a truncated multipole expansion retaining only dipole[31−34] and quadrupole terms.[9] Sokhan and Tildesley[9] showed that the early studies incorporated only dipole contributions, leading to the conclusion that the surface potential was positive (see Figure 1), whereas including the quadrupole contribution made the surface potential negative (see Figure 3). However, the effect of the higher multipole moments (octopole, hexadecapole, etc.)

on the surface potential was not investigated.[9] A multipole expansion is strictly valid[35] only when all of the multipole moments are included and when the test charge is located outside the spatial charge density. The spatial charge density computed from quantum mechanics includes all of the multipole moments and hence does not suffer from errors due to truncation of the multipole expansion. Ultimately, the manner in which the charge density is distributed throughout space must be determined from quantum mechanics.

Quantum mechanics has shown that electrons are distributed throughout matter in the attractive field of the atomic nuclei, with the real charge density being the sum of the nuclear and electronic charges (i.e., $\rho_{tot} = \rho_{nuc} + \rho_{elec}$). However, each molecular model of water has its own particular charge distribution chosen to mimic the real charge density. The great majority of molecular models for water[36−38] employ partial point charges (δ functions) at either the locations of the nuclei or elsewhere (e.g., patterned against the lone-pair orbitals of oxygen or to produce the gas-phase dipole and quadrupole moments; see Figure 3). These water models use partial charges that are much smaller than the bare nuclear charges because the nuclei are "screened" by the electronic charge density. Some water models include point polarizable sites[38] within the molecule in addition to the partial charges. Still fewer water models use Gaussian charge distributions centered on the nuclei with associated polarizable sites. In the final analysis, such models are idealizations of the real charge distributions of condensed-phase water molecules. These idealizations are necessary because of computational limitations; however, they have served the purpose of simplifying complex phenomena in such a way as to provide useful conceptual insights. Moreover, in many cases these water models are quantitative for several properties of water, with the caveat that one must exclude those properties that went into their parametrization. Table 1 shows a comparison of the surface potentials χ for several water models.

In recent years, the structure and electric properties of the vapor−liquid interface have received considerable attention from both experiment and theory. Experimentally, the orientational ordering of the vapor−liquid interface has been probed by second harmonic generation[15] (SHG) and sum frequency spectroscopy[30] (SFS). The interpretation of the SHG data implies that the dipole moment of water points slightly toward the liquid

(29) Asthagiri, D.; Pratt, L. R.; Ashbaugh, H. S. *J. Chem. Phys.* **2003**, *119*, 2702.
(30) Richmond, G. L. *Chem. Rev.* **2002**, *102*, 2693.
(31) Aloisi, G.; Guidelli, R.; Jackson, R. A.; Clark, S. M.; Barnes, P. *J. Electroanal. Chem.* **1986**, *206*, 131.
(32) Christou, N. I.; Whitehouse, J. S.; Nicholson, D.; Parsonage, N. G. *Mol. Phys.* **1985**, *55*, 397.
(33) Matsumoto, M.; Kataoka, Y. *J. Chem. Phys.* **1988**, *88*, 3233.
(34) Barraclough, C. G.; McTigue, P. T.; Ng, Y. L. *J. Electroanal. Chem.* **1992**, *329*, 9.

(35) Jackson, J. D. *Classical Electrodynamics*; John Wiley & Sons: New York, 1962.
(36) Berendsen, H. J. C.; Grigera, J. R.; Straatsma, T. P. *J. Phys. Chem.* **1987**, *91*, 6269.
(37) Jorgensen, W. L.; Chandrasekhar, J.; Madura, J. D.; Impey, R. W.; Klein, M. L. *J. Chem. Phys.* **1983**, *79*, 926.
(38) Dang, L. X.; Chang, T.-M. *J. Chem. Phys.* **1997**, *106*, 8149.

phase. The SFS data show the presence of free OH bonds. The value of χ (including both sign and magnitude) has been estimated from electrochemical measurements of $d\chi/dT$ using the fact that χ must vanish at the critical temperature, $T_c = 647$ K. From experiment, $d\chi/dT = -0.27$ mV/K at 298 K. Assuming a linear temperature dependence gives $\chi = +0.1$ V $= +100$ mV. The assumption of linearity underlies the view that the interfacial ordering of water molecules decreases linearly from its amount at 298 K to zero at T_c. However, using molecular dynamics simulations with the SPC/E water model, Sokhan and Tildesley[9] showed that $d\chi/dT$ depends nonlinearly on temperature, starting with a negative value at 298 K and then turning positive (for $T > 500$ K) as T approaches T_c. They found that $d\chi/dT = -1.0$ mV/K near 298 K, which is consistent with the measured $d\chi/dT$ value of -0.27 mV/K. Sokhan and Tildesley's surface potential for SPC/E is $\chi = -546$ mV at 298 K. This shows that χ can be negative and still have a negative value of $d\chi/dT$ near room temperature; however, $d\chi/dT$ passes through zero and then becomes positive as T_c is approached. The orientational averaging revealed two distinct layers with different structures: (1) the dipoles (or C_{2v} axis) on the vapor side of the Gibbs dividing surface are tilted toward the vapor phase at an angle of 78° to the surface normal, and (2) the dipoles on the liquid side of the Gibbs dividing surface (see Figure 3) are tilted slightly toward the liquid phase at an angle of 98° to the surface normal (other molecular studies[9,39,40] have found similar orientations through the interface). Their analysis of the nonlinear susceptibility showed that the two distinct layers contribute with opposite signs to the integral susceptibility, with the dominant contribution coming from the liquid side of the Gibbs dividing surface (i.e., where the dipole points slightly toward the liquid phase). Sokhan and Tildesley state that their surface potential χ should be considered as a lower limit because of the neglect of explicit polarization in the water model. Furthermore, they state that inclusion of polarization effects should result in an interfacial electric field that is dramatically weaker, since polarization works against the inducing field. However, the polarizable water model of Dang and Chang gives a χ value of -480 to -500 mV at 298 K[4,41] and a $d\chi/dT$ value of -1.2 mV/K from 298 to 323 K,[41] which are consistent with Sokhan and Tildesley's calculations and experiment. Other molecular studies[9] of the surface potential have found consistent results, which are displayed in Table 1 for comparison. Recently, Krishtalik[42] estimated χ using the thermodynamic approach in conjunction with the Born model of ion solvation. He found a positive value for χ ($+140$ mV) but cautions that his approach involved a number of assumptions and cannot be considered as rigorously quantitative. In particular, the Born model treats the water as a continuum dielectric[43] and thus does not contain atomistic and electronic degrees of freedom that are necessary to properly describe the essential physics.

The sensitivity of the surface potential χ has been discussed in the pioneering studies of Wilson, Pohorille, and Pratt.[6,7] They obtained $\chi = -130$ mV at 325 K using the TIP4P model and calculated the influence of the following on χ: (1) a modification

of the TIP4P water model's partial point charges (of the M sites) into Gaussian distributions and (2) a Gaussian fit of the electronic distribution of a single water monomer based on HF/6-31G** electronic structure data. From this study they concluded the following: "The surface potential is sensitive to details of the large distance wings of the molecular charge distribution."

In this paper, we present ab initio MD results for the surface potential χ at the vapor−liquid interface obtained directly from the total charge density $\rho_{tot} = \rho_{nuc} + \rho_{elec}$. In section II we discuss our methods and computational details, and in section III we present and then discuss the results. Finally, in section IV we close with conclusions and suggested directions for future research.

II. Methods and Computational Details

Previously,[44,45] the vapor−liquid interface was simulated using the simulation package CPMD[46] via a slab configuration containing 216 water molecules in a simulation cell of $15 \times 15 \times 71.44$ Å at $T = 298$ K. A total of 7 ps (starting from a previously equilibrated trajectory) was generated using the Car−Parrinello approach,[47] using a time-step of 0.097 fs with a fictitious mass of 400 au for the electronic degrees of freedom. The potential used was based on the Kohn−Sham formulation of density functional theory, in which plane waves expanded up to 70 Ry were used as the basis set in conjunction with Martins−Troullier pseudopotentials[48] to account for the core states. Gradient-corrected exchange and correlation functionals as parametrized by Becke[49] and Lee−Yang−Parr[50] (BLYP) were used because of their general success with hydrogen-bonded systems (future work will explore other functionals). Individual Nosé−Hoover thermostats[51,52] with a frequency of 3800 cm^{-1} were attached to every degree of freedom to ensure thermal equilibrium at 298 K. Decoupling of the periodic images in the z direction was performed as described by Mortensen and Parrinello[24] in conjunction with a large amount of vacuum (35 Å) to ensure convergence of surface properties.

For analysis, averaging was performed every 100 steps using the QuickStep module within CP2K,[53,54] which has been shown elsewhere to give structural and dynamical properties of water that are equivalent to those obtained from CPMD.[54] Unlike CPMD, CP2K utilizes a dual basis set of Gaussian-type orbitals (GTOs) and a plane-wave basis.[55] Specifically, we utilized a triple-ζ plus double polarization (TZV2P) GTO basis set and a smaller single-ζ (SZV) GTO basis to test basis-set dependence. For all of the runs, the density was expanded up to 280 Ry for the valence states, and dual-space GTH pseudopotentials[56] were used to account for the core states. It should be pointed out that the TZV2P basis set used in this study has been shown to closely reproduce the CPMD forces along identical trajectories.[54] Although this cannot be said about the use of the SZV basis, it was utilized in this study to provide a benchmark for the basis-set effects on the value of the surface

(39) Taylor, R. S.; Dang, L. X.; Garrett, B. C. *J. Phys. Chem.* **1996**, *100*, 11720.
(40) Wick, C. D.; Kuo, I-F. W.; Mundy, C. J.; Dang, L. X. *J. Chem. Theory Comput.* **2007**, *3*, 2002.
(41) Wick, C. D.; Dang, L. X.; Jungwirth, P. *J. Chem. Phys.* **2006**, *125*, 024706.
(42) Krishtalik, L. I. *Russ. J. Electrochem.* **2008**, *44*, 43.
(43) Kathmann, S. M.; Schenter, G. K.; Garrett, B. C. *Phys. Rev. Lett.* **2005**, *94*, 116104.
(44) Kuo, I-F. W.; Mundy, C. J. *Science* **2004**, *303*, 658.
(45) Kuo, I-F. W.; Mundy, C. J.; Eggimann, B. L.; McGrath, M. J.; Siepmann, J. I.; Chen, B.; Vieceli, J.; Tobias, D. J. *J. Phys. Chem. B* **2006**, *110*, 3738.
(46) CPMD; http://www.cpmd.org.
(47) Car, R.; Parrinello, M. *Phys. Rev. Lett.* **1985**, *55*, 2471.
(48) Troullier, N.; Martins, J. L. *Phys. Rev. B* **1991**, *43*, 1993.
(49) Becke, A. D. *Phys. Rev. A* **1988**, *38*, 3098.
(50) Lee, C.; Yang, W.; Parr, R. G. *Phys. Rev. B* **1988**, *37*, 785.
(51) Nosé, S. *J. Chem. Phys.* **1984**, *81*, 511.
(52) Hoover, W. G. *Phys. Rev. A* **1985**, *31*, 1695.
(53) CP2K; http://cp2k.berlios.de.
(54) VandeVondele, J.; Krack, M.; Mohamed, F.; Parrinello, M.; Chassaing, T.; Hutter, R. *Comput. Phys. Commun.* **2005**, *167*, 103–128.
(55) Lippert, G.; Hutter, J.; Parrinello, M. *Mol. Phys.* **1997**, *92*, 477.
(56) Goedecker, S.; Teter, M.; Hutter, J. *Phys. Rev. B* **1996**, *54*, 1703.

potential. The electronic states were quenched to a tolerance of 10^{-7} hartree.

The surface potential was directly determined from the real-space electrostatic potential obtained from the nuclear and electronic densities [$\rho_{tot}(\mathbf{r}) = \rho_{nuc}(\mathbf{r}) + \rho_{elec}(\mathbf{r})$, where $\mathbf{r}$ is the position vector to a point in real space]. The resulting real-space electrostatic potential is manifestly periodic through its Fourier space representation $\hat{V}_\mathbf{g}^H = 4\pi\hat{\rho}_\mathbf{g}^{tot}/g^2$, where $\hat{V}_\mathbf{g}^H$ and $\hat{\rho}_\mathbf{g}^{tot}$ represent the Hartree potential and total density, respectively, in Fourier space and g is the magnitude of the reciprocal lattice vector $\mathbf{g}$. It is important to note that the total charge density $\hat{\rho}_\mathbf{g}^{tot}$ integrates to zero, indicating that we are indeed studying a neutral aqueous system. The real-space Hartree potential $V^H(\mathbf{r})$ was obtained by a numerical Fourier transformation of $\hat{V}_\mathbf{g}^H$ and represented in units of hartree/e on an $N_x \times N_y \times N_z$ real-space grid with $N_x = N_y = 160$ and $N_z = 720$ determined by the density cutoff in CP2K. To obtain the electrostatic potential along the interfacial coordinate z, a simple averaging over the x and y directions was performed, namely,

$$V^H(\mathbf{r}) \Rightarrow V^H_{x,y,z} \tag{5}$$

and

$$V^H_z(z) = \varphi(z) = \frac{\sum\limits_{x,y} V^H_{x,y,z}}{N_x N_y} \tag{6}$$

As previously mentioned, the limits of integration on the z coordinate were taken to be positive as one moves from the vapor ($z_{outer} = 0$ Å) to the liquid phase ($z_{inner} = 35.7$ Å).

It is important to point out that $\rho_{nuc}(\mathbf{r})$ was computed within the pseudopotential approximation. This approximation introduces an inherent coarse-graining into the nuclear charge density that is mathematically modeled within the Ewald construction in order to avoid dealing with δ-function point charges at the nuclear sites. In the implementation in CP2K, it is this smoothed density that is chosen to represent the contribution of the nuclear charge density.[53] Thus, there is an additional contribution to the electrostatic potential that is due to the overlap of the charge densities. In the present application, the overlap contribution was essentially zero (e.g., $\sim10^{-6}$ hartree) and therefore not explicitly calculated. Thus, the electrostatic potential due to the nuclear degrees of freedom should be thought of as an average potential felt by a test charge and is not the δ-function nuclear potential. The assumption of the pseudopotential approximation was spot-checked with the electrostatic potential using the all-electron method of the Gaussian augmented plane-wave (GAPW) approach as implemented in CP2K.[57,58] In this calculation, a 6-31G** all-electron basis set was used. Within the GAPW approximation implemented in CP2K, the contribution to the potential due to $\rho_{nuc}(\mathbf{r})$ that is computed on the real-space grid is again a coarse-grained approximation to the δ-function nuclear charge density. Within the GAPW calculation, the resulting electrostatic potential is a smoothed representation of the true electrostatic potential.[57,58] Results from the GAPW calculations are in good agreement with the pseudopotential calculations and are used herein.

III. Results and Discussion

The computed electrostatic potential $\varphi(z)$ is presented in Figure 4, which shows the effect of using two different basis sets (TZV2P and SZV). The results for the two free interfaces were averaged to produce a single surface potential profile running from the center of the simulation cell to the vacuum. The two basis sets yield very consistent results for the surface
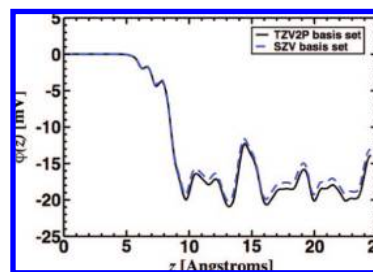
(57) Lippert, G.; Hutter, J.; Parrinello, M. *Theor. Chem. Acc.* **1999**, *103*, 124.
(58) Iannuzzi, M.; Chassaing, T.; Wallman, T.; Hutter, J. *Chimia* **2005**, *59*, 499.

Figure 4. Comparison of the electrostatic potentials $\varphi(z)$ (mV) as a function of z obtained using two different basis sets: TZV2P (solid black) and SZV (dashed blue).
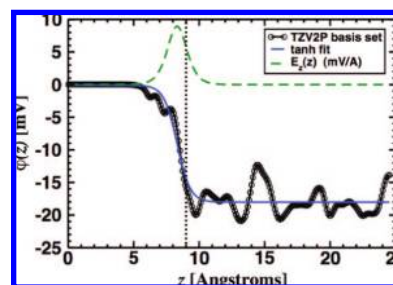

Figure 5. TZV2P data for the electrostatic potential $\varphi(z)$ (black circles) along with a tanh fit to the $\varphi(z)$ data (smooth solid blue curve) and the corresponding interfacial electric field $E_z(z)$ (dashed green curve). The Gibbs dividing surface (GDS) is located at $z = 9$ Å (vertical dotted line).

potential χ, but the SZV results are about 1 mV smaller than the TZV2P results. The remainder of the analysis will use the surface potential results from the TZV2P basis set. The TZV2P $\varphi(z)$ data (black circles) are shown in Figure 5 along with a tanh fit to the $\varphi(z)$ data (smooth solid blue curve) and the corresponding interfacial electric field $E_z(z)$ (dashed green curve). In Figure 5, the Gibbs dividing surface (GDS) is located at $z = 9$ Å (vertical dotted line). We arbitrarily define the GDS to be located where the mass density is equal to half that of the bulk liquid. The tanh fit was performed using the function

$$\varphi(z) = c_1 \tanh(z + c_2) + c_3 \tag{7}$$

where $c_1 = -8.9704$, $c_2 = -19.318$, and $c_3 = -9.0579$ are constants determined by a least-squares fit. The tanh fit to the CP2K/TZV2P results yields a surface potential of $\chi = -18$ mV. The use of the tanh functional form only approximates the data, but without theoretical justification for other functional forms, we feel that it provides as reasonable approximation to the raw $\varphi(z)$ data. Moreover, the influence of this choice on the E-field calculation is small. Table 1 shows a comparison of our surface potential with those found using other water models.[9] As mentioned previously, the results to date from molecular simulations have uniformly found a consistent sign (negative) and magnitude (hundreds of millivolts) for χ. This is consistent with the water molecules on the vapor side of the GDS having their hydrogen atoms pointing toward the vapor phase, giving rise to the positive sign of the electric field. However, our result of $\chi = -18$ mV is ~28 times smaller than the value of -500 mV found using an empirical polarizable interaction potential[40,41] for water. It should be noted that our hydrogen-bond populations are consistent with a variety of empirical (both fixed-charge and polarizable) interaction potentials.[40,45] The interfacial electric field was found by numerical differentiation (centered-difference): $E_z(z) = -[d\varphi(z)/dz]\hat{z}$. We obtain a maximum in the interfacial electric field of $[E_z(z)]_{max} = 8.9 \times 10^7$ V/m, which is ~15 times smaller than the value of 1.4×10^9 V/m found
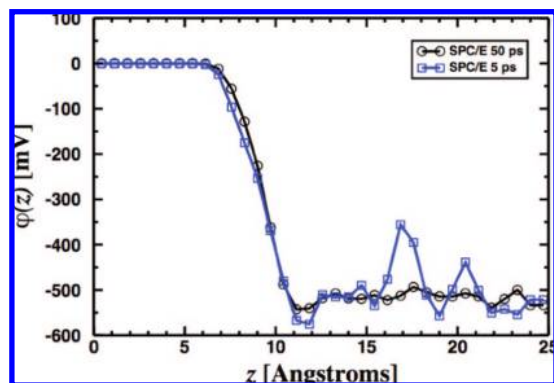
Figure 6. The SPC/E water model electrostatic potential $\varphi(z)$ for 50 ps (black circles) and 5 ps (blue squares).

using an empirical polarizable water model.[40,41] It should be noted that the interfacial electric field peaks on the vapor side of the GDS (~1 Å to the left of the GDS in Figure 5). These results are entirely consistent with those from the previous investigations of Pratt et al.[12] and Sokhan and Tildesley[9] and the SHG[15] and SFS[30] experiments indicating the presence of free OH bonds. Pratt et al. and Sokhan and Tildesley have both indicated the importance of incorporating the appropriate charge distributions (electronic and nuclear) into the condensed-phase and interfacial regions—here lies the true strength of accurate electronic structure methods. From the surface potential, the width of the interfacial region is ~5 Å. The full width at half-maximum of the interfacial electric field is ~2 Å (i.e., approximately the width of a water molecule).

To test the convergence of our CP2K/BLYP results using a 7 ps trajectory, we ran the same size system (216 water molecules) using the SPC/E water model[59] for a total of 50 ps and compared the convergence and fluctuations resulting from averaging over 5 and 50 ps (see Figure 6). These results show that our 7 ps trajectory is sufficient to quantify the surface potential. Even though the 5 ps SPC/E trajectory has larger fluctuations than the 50 ps trajectory, the magnitude of the surface potential can still be calculated. The SPC/E surface potential obtained in the present study ($\chi \approx -525$ mV) is consistent with the result from previous simulations by Sokhan and Tildesley[9] ($\chi = -546$ mV) using 500 water molecules for 4 ns.

As mentioned previously, the determination of the surface potential χ allows the real potential $\alpha_i = \mu_i + z_i\chi$ to be partitioned into chemical (μ_i) and electric ($z_i\chi$) contributions. Using our χ value of -18 mV, we find the electric contribution to the real potential from a univalent ion ($z_i = 1e$) to be -0.42 kcal/mol, which is considerably smaller than previous estimates of -11.53 kcal/mol obtained using a typical χ value of -500 mV. Thus, the electric contribution to the real potential utilizing a charge density obtained from electronic structure is much smaller than those from previous studies on the vapor–liquid interface of water. As an example (see Asthagiri et al.[29]), two recent estimates for the free energy of a proton in water can be considered: (1) Tissandier et al.[60] (T) obtained $\alpha^T[H^+] = -263.98$ kcal/mol and (2) Zhan and Dixon[61] (ZD) found $\alpha^{ZD}[H^+] = -262.4$ kcal/mol. Asthagiri et al. concluded that the free energies of T (and similarly ZD) include the contribution

of the reversible work against the surface potential, contrary to the conventional interpretation of these quantities. Assuming that Asthagiri et al. are correct in their interpretation and using our value ($\chi = -18$ mV) for the surface potential yields $\mu^T[H^+] = -263.57$ kcal/mol and $\mu^{ZD}[H^+] = -262.0$ kcal/mol, respectively. Ultimately, the exact interpretation of these quantities and how they relate to the extrathermodynamic assumption will only be resolved with additional computational studies.[62] Future work will address the following: (1) calculation of $d\chi/dT$ and how this quantity varies as T approaches the critical temperature T_c; (2) the dependence of χ on water cluster size and temperature (i.e., $\chi_i(T) = \chi[(H_2O)_i, T]$ for $i = 1$ to bulk) to study how the surface potential converges to the bulk value at the vapor–liquid interface of pure water.

IV. Conclusions

We have presented the first computation of the surface potential χ of water using ab initio molecular dynamics. We have found that the surface potential is $\chi = -18$ mV with a maximum interfacial electric field $[E_z(z)]_{max} = 8.9 \times 10^7$ V/m. A comparison was made between our quantum-mechanical results and those from previous molecular simulations, under-scoring the different treatments of the charge distributions (multipole expansions using dipole and quadrupole moments, partial point charges with and without polarizability, and quantum-mechanical electronic structure). We have found that explicit treatment of the electronic density makes a dramatic contribution to the electric properties of the vapor–liquid interface of water, consistent with the conclusions of Sokhan and Tildesley[9] and Pratt et al.[12] The E field can alter interfacial reactivity and transport, while the surface potential can be used to determine the "chemical" contribution to the real and electrochemical potentials for ion transport through the vapor–liquid interface. Future studies will address the surface potential and electric field at the interface between a salt crystal and liquid water as well as electronic effects on the potential of mean force of various ions through the vapor–liquid interface of water.

(59) Berendsen, H. J. C.; Grigera, J. R.; Straatsma, T. P. *J. Phys. Chem.* **1987**, *91*, 6269.

(60) Tissandier, M. D.; Cowen, K. A.; Feng, W. Y.; Gundlach, E.; Cohen, M. H.; Earhart, A. D.; Coe, J. V.; Tuttle, T. R. J. *J. Phys. Chem. A* **1998**, *102*, 7787.

(61) Zhan, C.-G.; Dixon, D. A. *J. Phys. Chem. A* **2001**, *105*, 11534.

(62) Kelly, C. P.; Cramer, C. J.; Truhlar, D. G. *J. Phys. Chem. B* **2007**, *111*, 408.